Oncogenic H-Ras reprograms Madin-Darby canine kidney (MDCK) cell-derived exosomal proteins following epithelial-mesenchymal transition

Bow J. Tauro[1, 2#], Rommel A. Mathias[1, 3#], David W. Greening[1], Shashi K. Gopal[1], Hong Ji[1], Eugene A. Kapp[4], Bradley M. Coleman[5], Andrew F. Hill[5], Ulrike Kusebauch[6], Janice L Hallows[6], David Shteynberg[6], Robert L. Moritz[6], Hong-Jian Zhu[7], and Richard J. Simpson[1*]

[1] Department of Biochemistry, La Trobe Institute for Molecular Science, La Trobe University, Bundoora, Victoria, Australia

[2] Department of Biochemistry and Molecular Biology, The University of Melbourne, Parkville, Victoria, Australia.

[3] Current address: Department of Molecular Biology, Princeton University, Princeton, New Jersey, U.S.A.

[4] The Walter and Eliza Hall Institute of Medical Research, Parkville, Victoria, Australia

[5] Department of Biochemistry and Molecular Biology, Bio21 Molecular Science and Biotechnology Institute, The University of Melbourne, Parkville, Victoria, Australia.

[6] Institute for Systems Biology, 401 Terry Ave North, Seattle, WA, USA. 98109-5234.

[7] Department of Surgery, Royal Melbourne Hospital, The University of Melbourne, Parkville, Victoria, Australia

[#] These authors contributed equally to this work

*** To whom correspondence should be addressed:**

Professor Richard J. Simpson

La Trobe Institute for Molecular Science (LIMS)

Room 113, Physical Sciences Building 4, La Trobe University

Bundoora, Victoria 3086, Australia

Tel: +61 3 9479 3099

Running title: Exosomes in EMT

Keywords: Epithelial-mesenchymal transition, EMT, MDCK, Ras, Exosomes, Proteomics, Splicing factor, Transcription factor

ABBREVIATIONS

21D1, Ras-transformed MDCK cells

21D1-Exos, Ras-transformed MDCK cell-derived exosomes

ADAM, a disintegrin and metalloproteinase

CM, culture medium

CCM, concentrated culture medium

DMEM, Dulbecco's Modified Eagle's Medium

EM, electron microscopy

EMT, epithelial-mesenchymal transition

EVs, extracellular vesicles

FCS, fetal calf serum

MDCK, Madin-Darby canine kidney

MDCK-Exos, Madin-Darby canine kidney derived exosomes

MMP, matrix metalloproteinase

MVB, multivesicular body

NMWL, nominal molecular weight limit

Rsc, relative spectral count fold change ratio

TEM, transmission electron microscopy

YBX1, Y-box binding protein 1

ABSTRACT

Epithelial-mesenchymal transition (EMT) is a highly conserved morphogenic process defined by the loss of epithelial characteristics and the acquisition of a mesenchymal phenotype. EMT is associated with increased aggressiveness, invasiveness, and metastatic potential in carcinoma cells. To assess the contribution of extracellular vesicles following EMT, we conducted a proteomic analysis of exosomes released from Madin-Darby canine kidney (MDCK) cells, and MDCK cells transformed with oncogenic H-Ras (21D1 cells). Exosomes are 40-100 nm membranous vesicles originating from the inward budding of late endosomes and multivesicular bodies (MVBs) and are released from cells upon fusion of MVBs with the plasma membrane. Exosomes from MDCK cells (MDCK-Exos) and 21D1 cells (21D1-Exos) were purified from cell culture media using density gradient centrifugation (OptiPrep™), and protein content identified by GeLC-MS/MS proteomic profiling. Both MDCK- and 21D1-Exos populations were morphologically similar by cryo-electron microscopy and contained stereotypical exosomes marker proteins such as TSG101, Alix and CD63. In this study we show that the expression levels of typical EMT hallmark proteins seen in whole cells correlate with those observed in MDCK- and 21D1-Exos – i.e., reduction of characteristic inhibitor of angiogenesis, thrombospondin-1 and epithelial markers E-cadherin, and EpCAM, with a concomitant up-regulation of mesenchymal makers such as vimentin. Further, we reveal that 21D1-Exos are enriched with several proteases (e.g., MMP-1, -14, -19, ADAM-10, ADAMTS1), and integrins (e.g., ITGB1, ITGA3, ITGA6) that have been recently implicated in regulating the tumour microenvironment to promote metastatic progression. A salient finding of this study was the unique presence of key transcriptional regulators (e.g., the master transcriptional regulator YXB1) and core splicing complex components (e.g., SF3B1, SF3B3 and SFRS1) in mesenchymal 21D1-Exos. Taken together, our findings reveal

that exosomes from Ras-transformed MDCK cells are reprogrammed with factors which may be capable of inducing EMT in recipient cells.

INTRODUCTION

Epithelial-mesenchymal transition (EMT) is a cellular process whereby otherwise sessile epithelial cells undergo a shift in plasticity and acquire the ability to disseminate [1-6]. Hallmarks of EMT include diminished expression of cell-cell contact/adhesion components (e.g., E-cadherin), diminished expression of cell-matrix components, decreased expression of components involved in cell polarity, elevated expression of proteins involved in cytoskeleton remodelling (e.g., vimentin), and increased expression of various matrix metalloproteinases [7]. Established as a central process during the early stages of development [8, 9], EMT also has implications in wound healing, fibrosis and, more recently, cancer progression [10-12]. In the latter, EMT is thought to promote metastasis by triggering invasive and anti-apoptotic mechanisms in tumour cells, stimulate the cancer stem cell phenotype, and activate the tumour microenvironment via structural and biochemical modifications [13]. Although, crosstalk between numerous intracellular signalling pathways are known to regulate EMT [14], it is now emerging that the EMT process can modulate the tumour microenvironment [15].

The complexity of the tumour microenvironment goes far beyond occupant epithelial cancer cells containing several non-malignant, albeit genetically altered, heterotypic cell types (e.g., fibroblasts, endothelial cells and immune cells) [16]. Crosstalk is possible, either physically or via secretion of components such as extracellular matrix (ECM) proteins, enzymes, or paracrine signalling molecules such as growth factors and inflammatory cytokines (collectively referred to as the secretome) [17-19]. Given that cancer cells at the leading tumour edge can undergo EMT and initiate metastatic lesion formation in response to signals from the microenvironment [11, 20], considerable effort has been directed towards

characterising the tumour secretome [21, 22]. To identify extracellular modulators of EMT which may influence tumour cell state and invasive potential, we have previously analysed the secretome (soluble secreted proteins) from Madin-Darby canine kidney (MDCK) and Ras-transformed MDCK (21D1) cells [23, 24]. This proteomic-based approach enabled an unbiased global overview of events occurring in the extracellular microenvironment. The expression of components mediating cell-cell and cell-matrix adhesion (collagen XVII, IV, and laminin 5) were attenuated, with concordant up-regulation of proteases and ECM constituents promoting cell motility and invasion (MMP-1, TIMP-1 kallikrein-6, -7, fibronectin, collagen I, fibulin-1, -3, biglycan, decorin, S100A4 and SPARC) [23, 24]. It is becoming increasingly clear that in addition to the soluble-secreted cytokines and chemokines that mediate cell communication at primary and secondary tumour sites [25], extracellular membranous vesicles, including exosomes, are important regulators of the tumour microenvironment [19, 26, 27].

Extracellular vesicles (EVs) are capable of enhancing the invasive potential of breast cancer and induce angiogenesis and metastasis in lung cancer [28, 29]. In addition, transfer of oncogenic potential to a recipient cell through activation of MAPK and Akt signalling pathways highlights new mechanisms of intercellular communication via EVs in the tumour microenvironment [30, 31]. EVs can be categorised by size with apoptotic bodies ranging up to 4000 nm in diameter, shed microvesicles/ectosomes 100-1000 nm, and 40-100 nm exosomes [32, 33]. Importantly, exosomes have been associated with modulating the immune response, controlling tumour stroma in the metastatic niche, activating signalling pathways and transferring genetic and oncogenic information to neighbouring cells [32, 34-38]. Although many functional activities have been ascribed to exosomes, it should be noted that the majority of sample preparations used for functional studies are heterogeneous in

nature containing several EV types including shed microvesicles, exosomes and apoptotic blebs. As a first step towards characterising the specific contribution of exosomes to the tumour microenvironment, we report in this study the first protein analysis of highly-purified exosomes before and after the EMT process. Comparison of MDCK exosome protein profiles following oncogenic Ras-induced EMT revealed extensive reprogramming in favour of components promoting metastatic niche formation. Additionally, enrichment of transcription and splicing factors known to induce EMT were observed in 21D1 exosomes, suggesting that a recipient cell may undergo EMT following exosome uptake.

EXPERIMENTAL PROCEDURES

Cell culture and CCM preparation - MDCK cells [39] and oncogenic H-Ras-transformed MDCK derivative 21D1 cells [23, 24] were routinely cultured in Dulbecco's modified Eagle's medium (DMEM) (Life Technologies, NY, USA) supplemented with 10% FCS (Life Technologies), at 37 ºC with 10% CO_2. MDCK and 21D1 cells were grown to 70% confluence in DMEM containing 10% FCS, washed three times with serum-free DMEM, and left to culture in this medium at 37 ºC with 10% CO_2 for 24 h. Culture medium (CM) from 60 dishes of each cell line (a total of 900 mL from approximately 3×10^8 cells) was harvested and centrifuged twice (480 × *g* 5 min, 2000 × *g* 10 min) to sediment floating cells and remove cellular debris. CM was centrifuged at 10,000 × *g* for 30 min to remove shed microvesicles. The resultant supernatant was filtered using a VacuCap® 60 filter unit fitted with a 0.1 µm Supor® Membrane (Pall Life Sciences, Port Washington, NY) and then concentrated to 1 mL concentrated culture medium (CCM) using Amicon® Ultracel-15 centrifugal filter devices with a 5K nominal molecular weight limit (NMWL) (Merck-Millipore, MA, USA).

Exosome isolation using OptiPrep™ density gradient - Exosomes were isolated as previously described [40]. Briefly, to prepare the discontinuous iodixanol gradient, 40% (w/v), 20% (w/v), 10% (w/v) and 5% (w/v) solutions of iodixanol were made by diluting a stock solution of OptiPrep™ (60% (w/v) aqueous iodixanol from Axis-Shield PoC, Norway) with 0.25 M sucrose/10 mM Tris, pH 7.5. The gradient was formed by adding 3 mL of 40% iodixanol solution to a 14 × 89 mm polyallomer tube (Microfuge® Tube, Beckman Coulter), followed by careful layering of 3 mL each of 20% and 10% solutions, and 2 mL of the 5% solution. For each exosome preparation, CCM (1 mL) was overlaid on the gradient, and centrifugation performed at 100,000 × g for 18 h at 4 ºC. Twelve individual 1 mL gradient fractions were collected manually (with increasing density). Fractions were diluted with 2 mL PBS and centrifuged at 100,000 × g for 3 h at 4 ºC followed by washing with 1 mL PBS, and resuspended in 50 µL PBS. Fractions were monitored for the expression of exosomal markers Alix and TSG101 by Western blotting. To determine the density of each fraction, a control OptiPrep™ gradient containing 1 mL of 0.25 M sucrose/10 mM Tris, pH 7.5 was run in parallel. Fractions were collected as described, serially diluted 1:10,000 with water, and the iodixanol concentration determined by absorbance at 244 nm using a molar extinction coefficient of 320 L $g^{-1}cm^{-1}$ [41].

Protein quantitation - The protein content of exosome preparations was estimated by 1D-SDS-PAGE / SYPRO® Ruby protein staining densitometry. This method is reproducible, has a linear quantitation range over three orders of magnitude [42], and is compatible with GeLC-MS/MS [43]. Briefly, 5 µL sample aliquots were solubilised in SDS sample buffer (2% (w/v) sodium dodecyl sulfate, 125 mM Tris-HCl, pH 6.8, 12.5% (v/v) glycerol, 0.02% (w/v) bromophenol blue) and loaded into 1 mm, 10-well NuPAGE™ 4-12% (w/v) Bis-Tris

Precast gels (Life Technologies), Electrophoresis was performed at 150 V for 1 h in NuPAGE™ 1 × MES running buffer (Life Technologies) using an XCell Surelock™ gel tank (Life Technologies). After electrophoresis, gels were removed from the tank and fixed in 50 mL fixing solution (40% (v/v) methanol, 10% (v/v) acetic acid in water) for 30 min on an orbital shaker and stained with 30 mL SYPRO® Ruby (Life Technologies, NY, USA) for 30 min, followed by destaining twice in 50 mL of 10% (v/v) methanol with 6% (v/v) acetic acid in water for 1 h. Gels were imaged on a Typhoon 9410 variable mode imager (Molecular Dynamics, Sunnyvale, USA), using a green (532 nm) excitation laser and a 610BP30 emission filter at 100 µm resolution. Densitometry quantitation was performed using ImageQuant software (Molecular Dynamics) to determine protein concentration relative to a BenchMark™ Protein Ladder standard of known protein concentration (1.7 µg/µL) (Life Technologies). The yield of purified exosomes was ~60 µg from 3×10^8 cells for both MDCK- and 21D1-Exos.

Western blot analysis - Exosome samples (~10 µg protein) were prepared for Western blot analysis as previously described [44]. Membranes were probed with primary mouse anti-TSG101 (BD Transduction Laboratories; 1:500), mouse anti-Alix (Cell Signaling Technology; 1:1000), mouse anti-H-Ras (Santa Cruz Biotechnology; 1:500), mouse anti-E-cadherin (BD Transduction Laboratories; 1:1000), rabbit anti-EpCAM (Abcam, 1:1000), rabbit anti-MMP-1 (Santa Cruz Biotechnology; 1:200), rabbit anti-YB-1(YBX1) (Abcam; 1:500) or mouse anti-vimentin (Merck-Millipore; 1:500), for 1 h in TTBS (50 mM Tris, pH 7, 150 mM NaCl, 0.05% (v/v Tween 20) followed by incubation with the secondary antibody, IRDye 800 goat anti-mouse IgG or IRDye 700 goat anti-rabbit IgG (1:15000, LI-COR Biosciences, Nebraska USA), for 1 h in darkness. All antibody incubations were carried out using gentle orbital shaking at RT. Western blots were washed three times in TTBS for 10

min after each incubation step and visualised using the Odyssey Infrared Imaging System, version 3.0 (LI-COR Biosciences,).

Cryo-electron microscopy - Purified MDCK-exosomes (MDCK-Exos) and 21D1-exosomes (21D1-Exos) were imaged using cryo-transmission electron microscopy (cryo-(EM)as previously described [39] with slight modifications. Briefly, Aurion Protein-G gold 10 nm (ProSciTech, QLD, Australia) was mixed at a 1:3 ratio with exosomes (2 µg) harvested from OptiPrep™ gradients suspended in PBS buffer and transferred onto glow-discharged C-flat holey carbon grids (ProSciTech). Excess liquid was blotted and grids were plunge-frozen in liquid ethane. Grids were mounted in a Gatan cryoholder (Gatan, Inc., Warrendale, PA, USA) in liquid nitrogen. Images were acquired at 300 kV using a Tecnai G2 F30 (FEI, Eidhoven, NL), in low dose mode.

GeLC-MS/MS - MDCK- and 21D1-Exos (20 µg) were lysed in SDS sample buffer, and proteins separated by SDS-PAGE and visualized by Imperial™ Protein Stain (Thermo Fisher Scientific), according to manufacturer's instructions. Gel lanes were cut into equal slices (20 × 2 mm) using a GridCutter (The Gel Company, San Francisco, CA) and individual gel slices were subjected to in-gel reduction, alkylation and trypsinization [45]. Briefly, gel bands were reduced with 10 mM DTT (Calbiochem, San Diego, USA) for 30 min, alkylated for 20 min with 25 mM iodoacetic acid (Fluka, St. Louis, USA), and digested with 150 ng trypsin (Worthington Biochemical Corp, Freehold, USA) for 4.5 h at 37 °C. Tryptic peptides were extracted with 50 µL 50% (v/v) acetonitrile, 50 mM ammonium bicarbonate, concentrated to ~10 µL by centrifugal lyophilisation and one technical replicate analysed by LC-MS/MS. RP-HPLC was performed on a nanoAcquity® (C18) 150 × 0.15-mm-internal diameter reversed phase UPLC column (Waters, Milford, USA) using an Agilent 1200 HPLC

coupled online to an LTQ-Orbitrap mass spectrometer equipped with a nanoelectrospray ion source (Thermo Fisher Scientific). The column was developed with a linear 60 min gradient with a flow rate of 0.8 µL/min at 45 °C from 0-100% solvent B where solvent A was 0.1% (v/v) aqueous formic acid and solvent B was 0.1% (v/v) aqueous formic acid/60% acetonitrile. Survey MS scans were acquired with the resolution set to a value of 30,000. Real time recalibration was performed using a background ion from ambient air in the C-trap [46]. Up to five selected target ions were dynamically excluded from further analysis for 3 min. An additional biological replicate of MDCK- and 21D1-Exos (20 µg) was analysed on an LTQ-Orbitrap mass spectrometer (**Supplemental Data**) to validate our primary findings. Raw mass spectrometry data is deposited in the PeptideAtlas and can be accessed at http://www.peptideatlas.org/PASS/PASS00225 [47-49].

Database searching and protein identification - Peak lists were extracted using *extract-msn* as part of Bioworks 3.3.1 (Thermo Fisher Scientific). The parameters used to generate the peak lists were as follows: minimum mass 700, maximum mass 5000, grouping tolerance 0.01 Da, intermediate scans 200, minimum group count 1, 10 peaks minimum and total ion current of 100. Peak lists for each LC-MS/MS run were merged into a single MGF file for Mascot searches. Automatic charge state recognition was used because of the high-resolution survey scan (30,000). MGF files were searched using the Mascot v2.2.01 search algorithm (Matrix Science) against the LudwigNR_Q410 database with a taxonomy filter for human, cow and dog, comprising 13112897 entries (http://www.ludwig.edu.au/archive/LudwigNR/LudwigNR.pdf). The search parameters consisted of carboxymethylation of cysteine as a fixed modification (+58 Da), NH_2-terminal acetylation (+42 Da) and oxidation of methionine (+16 Da) as variable modifications. A peptide mass tolerance of ±20 ppm, #13C defined as 1, fragment ion mass tolerance of ±0.8

Da, and an allowance was made for up to two missed tryptic cleavages. Protein identifications were firstly clustered and analysed by an in-house developed program *MSPro* [50]. Briefly, peptide identifications were deemed significant if the Ion score was ≥ the Homology score. False-positive protein identifications were estimated by searching MS/MS spectra against the corresponding reverse-sequence (decoy) database [50]. MDCK- and 21D1- exosome protein identifications were based on a protein score above the 1% false discovery rate cut-off of 48, and with at least 2 significant peptides. The BioMart data-mining tool (http://www.ensembl.org/biomart/index.html) was used to obtain Ensembl protein description and gene name as described [51]. UniProt (http://www.uniprot.org) and Protein Information Resource (http://pir.georgetown.edu) were used to obtain gene ontology (GO) annotation.

Semi-quantitative label-free spectral counting - Significant spectral count fold change ratios (R_{SC}) were determined using a modified formula from a previous serial analysis of gene expression study by Beissbarth *et al*. [52].

$$R_{SC} = (n_{21D1\text{-}Exos}+f)\,(t_{MDCK\text{-}Exos}-n_{MDCK\text{-}Exos}+f) \,/\, (n_{MDCK\text{-}Exos}+f)\,(t_{21D1\text{-}Exos}-n_{21D1\text{-}Exos}+f) \qquad \text{(Eq. 1)}$$

where, n is the significant protein spectral count (a peptide spectrum is deemed significant when the Ion score ≥ the Homology score), t is the total number of significant spectra in the sample, and f a correction factor set to 1.25 [53]. Total number of spectra was only counted for significant peptides identified (Ion score ≥ Homology score). When Rsc is less than 1, the negative inverse Rsc value was used. The number of significant assigned spectra for each protein was used to determine whether protein abundances between the two categories (MDCK- and 21D1-Exos). For each protein the Fisher's Exact test was applied to significant

assigned spectra. The resulting p-values were corrected for multiple testing using the Benjamini-Hochberg procedure [54] and computations carried out in R [55].

RESULTS AND DISCUSSION

Exosomes are released from MDCK cells following oncogenic H-Ras induced EMT - Previously, we established that cultured MDCK cells undergoing oncogenic H-Ras mediated EMT (21D1 cells) secrete protein components that extensively remodel the extracellular microenvironment - e.g., increased expression of ECM proteins - migration factors, and proteases that promote cell motility and invasion [23, 24]. MDCK cells exhibit cobblestone-like morphology while 21D1 cells displayed a spindle-shaped mesenchymal phenotype (**Fig. 1A**). To maintain the mesenchymal phenotype, 21D1 cells require co-culture with their own culture medium (**Supplemental Figure S1**). To isolate exosomes, MDCK and 21D1 cells were cultured to ~70% confluence, washed with DMEM, and then left to culture in serum-free medium for 24 h. We have previously shown that both cell lines remain greater than 96% viable during this time [23]. Culture medium (CM) from ~$3x10^8$ cells was harvested, concentrated (CCM) by centrifugal membrane ultrafiltration and crude exosomes were fractionated based upon their buoyant density into 12 fractions using iodixanol density gradient centrifugation [40] as outlined in **Fig. 1B**. Western blot analysis of these fractions revealed enrichment of exosomes (based on exosome markers Alix/PDCD6IP and TSG101) in a fraction with buoyant density 1.09 g/mL (**Fig. 2A, Supplemental Figure S2**). Interestingly, H-Ras was found in both MDCK- and 21D1-Exos, but with much higher levels in 21D1-Exos (**Fig. 2A**). The existence of H-Ras in the MDCK-Exos suggests that endogenously expressed Ras is implicated in secretory exosomal trafficking; however, it is not clear which form of H-Ras this is (inactive Ras-ADP or active Ras-ATP). Given that v-H-Ras expressed in 21D1 cells is the mutated active form, and that higher levels are observed in 21D1-Exos, it is suggestive of the involvement of the membrane-bound active Ras-ATP form in the secretory 21D1-Exos. This is consistent with the findings regarding K-Ras by

Demory Beckler et al., [56]. The yield of purified exosomes was ~60 µg from $3x10^8$ cells for both MDCK- and 21D1-Exos. Cryo-EM of purified exosomes revealed a relatively homogenous population of round membranous vesicles 40-100 nm in size, which is in accordance with the typical size reported for exosomes (**Fig. 2B**) [33].

(INSERT FIGURE 1 and 2)

Proteome analysis of MDCK- and 21D1-Exos - We next compared the protein profiles of MDCK- and 21D1-Exos using GeLC-MS-MS. Protein visualisation using Imperial™ Protein Stain indicates significant differences in MDCK- and 21D1-Exos protein profiles following oncogenic H-Ras induced EMT (**Fig. 3A**). GeLC-MS/MS profiling [45] identified a total of 458 proteins, comprising 382 and 401 in MDCK- and 21D1-Exos, respectively (**Fig. 3B** and **Supplemental Tables S1-3**). Of the 325 proteins common to both MDCK- and 21D1-Exos, many are involved in exosome biogenesis (e.g., proteins involved in the ***e***ndosomal ***s***orting ***c***omplex ***r***equired for ***t***ransport (ESCRT) machinery such as TSG101, VPS28, VPS37B, ESCRT accessory protein Alix [57]), coordination of intracellular vesicle trafficking (e.g., tetraspanins such as CD63 and CD9 [58, 59], small Rab GTPases such as RAB1B, RAB5A, RAB5B, RAB5C, RAB7A, RAB11A, RAB14, RAB21 [60-62]), and annexins such as ANXA1, ANXA2, ANXA4, ANXA7, ANXA8, ANXA11 [63]. 247 of the 325 common proteins (76%) have been reported by other researchers to be present in exosomes released from diverse cell types (see exosomes database ExoCarta containing 13,333 protein entries, Download 4 - release date: 29 May 2012 http://exocarta.org/index.html) [64, 65]. Overall, 139 of the 458 MDCK- and 21D1-Exos proteins identified in this study have not been reported in ExoCarta (**Supplemental Table S4**). According to GO subcellular annotation, 28 of these proteins are secreted, 12 cell

membrane, 12 membrane, and 4 lipid-anchor proteins. Protein CYR61 (CYR61) is involved in promoting cell proliferation, chemotaxis, angiogenesis and cell adhesion, while protein jagged-1 (JAG1), VEGFR-1 receptor (FLT1), MMP19, and ADAMTS1 involved in angiogenesis and signal transduction. Components involved in cell signalling include AP1M2, CD109, the COP9 signalosome complex protein subunit COPS3, and several tetraspanin proteins, such as TSPAN4 and TSPAN9 were identified. A biological replicate of MDCK- and 21D1-Exos revealed 88% (403/458) similarity in overall protein identifications (Supplemental Table 1).

(INSERT FIGURE 3)

EMT hallmark proteins are observed in exosomes upon oncogenic H-Ras induced EMT - We next examined whether the pattern of EMT hallmarks typically seen in whole cells [7] are reflected in exosomes released from MDCK cells following H-Ras modulated EMT. For this purpose we used relative spectral count ratios (Rsc) and Western immunoblotting to indicate differential protein expression between samples. Proteins mediating cell-cell contact, cell-matrix contact and cell polarity displayed decreased expression levels in 21D1-Exos (**Table 1** and **Fig. 2A**), correlating with typical EMT hallmarks seen in whole cells [7]. Foremost of these were the adhesive glycoprotein and inhibitor of angiogenesis thrombospondin 1 (THBS1 Rsc -482.8), and the epithelial cell markers E-cadherin (CDH1 Rsc -34.4) and EpCAM (Rsc -16.5). Consistent with these findings were the elevated protein expression levels in 21D1-Exos of vimentin (VIM, Rsc 8.1) and matrix metalloproteins, MMP-1 (Rsc 7.3), MMP-19 (Rsc 11.3) and MMP-14 (Rsc 3.4), typically observed in mesenchymal cells. Confirmatory data for the different abundance levels of CDH1, EpCAM, VIM, and MMP-1 observed in MDCK- and 21D1-Exos was obtained by Western blot analysis (**Fig. 2A**).

(INSERT TABLE 1)

Exosomes contain metastatic niche factors following oncogenic H-Ras-induced EMT - Melanoma-derived exosomes have been recently implicated in regulating the metastatic microenvironment in sentinel lymph nodes [27] and 'educating' circulating bone marrow progenitor cells to promote metastatic progression *in vivo* [66]. In contrast to MDCK-Exos, interrogation of the protein profile of 21D1-Exos revealed increased expression of proteases, annexins, integrins, and other secreted proteins associated with the pre-metastatic niche formation [19, 67-74], the tumour microenvironment [75] and proteins assisting tissue invasion and metastasis [76, 77] (**Table 2**).

Proteases - Proteases implicated in metastatic niche preparation and seen highly enriched in 21D1-Exos (relative to MDCK-Exos) include matrix metalloproteinases MMP-1 (Rsc 7.3), MMP-14 (Rsc 3.4), MMP-19 (Rsc 11.3), a disintegrin and metalloproteinase 10 (ADAM10) (Rsc 2.2), and ADAM with thrombospondin motif 1 (ADAMTS1) (Rsc 1.7). The interstitial collagenase MMP-1 is known to assist tumour-induced angiogenesis, tumour invasion, and establishment of metastatic regions at secondary sites [78]. Presence of MMP-1 in human colorectal carcinomas correlates with the depth grading of tumour invasion, lymphatic invasion, and lymph node metastasis [79]. MMP-14 promotes cell invasion and motility by pericellular ECM degradation, shedding of CD44 (also detected in 21D1-Exos) and syndecan 1, and through activation of ERK [80]. Expression of MMP-19 is associated with increased invasion, migratory behaviour and early metastasis of melanoma cells [81], and localisation of MMP-14 and -19 at the invasive tumour front is characteristic of highly-motile invading tumour cells [81, 82]. The finding that MMP-14 and -19 are unique to 21D1-

Exos and not observed in our previously published MDCK/21D1 secretome analysis [24], may represent a mechanism that allows exosome-bound proteases to traffic and function at distant/metastatic sites. ADAM proteases contain MMP-like catalytic domains [83] and are important mediators of cell surface protein shedding during tumour progression [84]. Interestingly, ADAM10 has been shown to be an active vesicle-based protease, cleaving cell adhesion molecule L1 at the cell surface, and subsequently promoting cell migration [85]. Given that other substrates of ADAM10 include components of the ECM, epidermal growth factors, chemokines, cytokines, and Notch receptor when bound to its ligands Delta-like 1 or Jagged-1 (also unique to 21D1-Exos, Rsc 4.9) [84], ADAM10 has the ability to extensively modify the tumour microenvironment. Likewise, ADAMTS1 is also capable of degrading various ECM components [86], and increased expression promotes pulmonary metastasis of mammary carcinoma and Lewis lung carcinoma cells [87]. ADAMTS1 has also been shown to modulate the metastatic tumour microenvironment by promoting angiogenesis and invasion in osteoclastogenesis [88]. These findings suggest that addition to soluble proteases, exosome-associated proteases ADAM10 and ADAMTS1 may also contribute to the EMT process [78] and, additionally, play a role in pre-metastatic niche formation [19].

Integrins – Integrins represent another class of metastatic niche components that were enriched in 21D1-Exos (**Table 2**). Integrins facilitate cell attachment to surrounding ECM, initiating intracellular signalling cascades that maintain cell survival, proliferation, adhesion, migration and invasion [89]. The finding of enriched protein levels of integrins in 21D1-Exos is of particular significance given that a study of ovarian carcinoma identified that collagen-induced activation of integrin receptors caused Ras, Erk and Akt pathway activation [90]. In particular, integrins subunits $\alpha 3$, $\alpha 6$, αV and $\beta 1$, all of which were enriched in 21D1-Exos, have been associated with modulating ECM-induced signalling leading to

proliferation, adhesion, migration and invasion of the ovarian cancer cells [90]. Moreover, αV mediates latent TGF-β activation, which is required for the maintenance of EMT and tumour cell invasion and dissemination [91]. These findings are in accord with our earlier studies showing plasma membrane bound integrins α6β1 and α3β1 were significantly enriched in cell membrane preparations of H-Ras transformed MDCK cells (21D1 cells) when compared to parental MDCK cells [51], further studies are required to ascertain whether these integrins are integral components of the 21D1-Exos membrane.

Tetraspanins –Tetraspanins are characterised by four transmembrane domains, intracellular N- and C-termini and two extracellular domains. They are reported to function as scaffolding proteins which interact with integrins; many tetraspanins have been implicated in tumour progression [92-94]. In this study, we observed an enrichment in 21D1-Exos of tetraspanins involved in cancer progression including CD81, CD82 and CD151 (**Table 2**). Interestingly, it has been previously shown that interactions between α6β1 (both integrin components identified in this study) and CD81 may up-regulate cell motility, affecting migration mediated by other integrins [95]. Recently, CD81-positive fibroblast-derived exosomes, isolated using differential ultracentrifugation, were reported to regulate breast cancer cell protrusions and motility through Wnt-planar cell polarity signalling [96]. Further, CD82 has been implicated in integrin-mediated functions including cell motility and invasiveness [97], while CD151 has been shown to promote cancer cell metastasis via integrins α3β1 and α6β1 (also seen in our study) *in vitro* [98].

Annexins - Annexins are involved in a diverse array of cellular functions and physiological processes including membrane scaffolding, trafficking and organization of vesicles, exocytosis, endocytosis and cell migration [99]. In this study, we observed

increased expression levels of annexins A1, A2, A4, A7, A8 and A11 (Rsc 1.3-2.3) in 21D1-Exos (**Table 2**). In particular, annexin A2 (Rsc 1.9), has been shown to regulate the tumour microenvironment by inducing the remodelling of cytoskeletal structures and actin of breast and colorectal cancer cells [100]. siRNA-based experiments have recently demonstrated that annexin A2 is critical in determining the invasive potential of cancer cells, and regulates secretion of pro-angiogenic factors including MMP-14 [101]. The precise functional roles played by other annexins during metastatic progression remain to be defined.

(INSERT TABLE 2)

Transcriptional regulators and splicing factors are enriched in exosomes following H-Ras-induced EMT - It is well recognized that splicing events and transcription regulation drive critical aspects of EMT–associated phenotypic change [102, 103]. For example, the EMT transcription factor *twist* altered global changes in mRNA splicing in a human mammary epithelial cell line (HMLE cells) resulting in many alternatively spliced genes that are implicated in processes such as cell migration, actin cytoskeletal regulation and cell–cell junction formation, all of which contribute to EMT phenotypic change [102]. We report, for the first time, the presence of key transcriptional regulators (e.g., the master transcriptional regulator YXB1) and core splicing complex components in highly-purified exosomes.

Splicing factors – Recent studies have highlighted an important contribution of alternative splicing to the metastatic cascade, including regulation of EMT at the post-transcriptional level [104, 105]. Alternative splicing results in the expression of protein isoforms with distinct structural and functional characteristics, and can even give rise to proteins with opposite properties [106]. The involvement of alternative splicing in EMT was

first reported in relation to the fibroblast growth factor receptor 2 (FGFR2) [107], and since then several splicing factors and spliced genes involved in cell migration, actin cytoskeletal regulation and cell–cell junction formation during EMT have been discovered [102, 108, 109]. Several splicing factors were identified in 21D1-Exos (**Table 3**) including the splicing regulator protein SRP20 (Rsc 2.7), and SF3B1 (Rsc 8.9) and SF3B3 (Rsc 2.6), which are components of the SF3b complex that interacts with U2 small nuclear ribonucleoprotein (snRNP) complex at the catalytic center of the spliceosome [110]. Increased expression levels of splicing factor, arginine/serine-rich 1 (SFRS1/SRSF1) (Rsc 23.2), previously known as (SF2/ASF), in 21D1-Exos is of particular significance given its ability to induce EMT [111]. SRSF1 has been shown to regulate the splicing of the tyrosine kinase receptor Ron which is synthesized as a single chain precursor, and is comprised of an extracellular 40 kDa α-subunit and a 145 kDa transmembrane β-subunit [112]. SRSF1 promotes the production of ΔRon 165 which is an isoform lacking 49 amino acids in the extracellular β-subunit generated through the skipping of exon 11 [111, 113]. ΔRon 165 is unable to undergo proteolytic processing and as a consequence accumulates in the cytoplasm in a constitutively phosphorylated form which induces invasive properties [114]. By these means, SRSF1 affects the Ron/ΔRon ratio, which in turn, promotes the morphological and molecular hallmarks of EMT [111]. SRSF1 is frequently up-regulated in various human tumours [115]. Our finding of the proto-oncogene SRSF1 in H-Ras induced 21D1-Exos may represent a mechanism by which a recipient cell upon uptake of an SRSF1-containing exosome may induce the recipient cell to undergo EMT. Further studies are required to examine this hypothesis.

Transcription factors – A salient finding of this analysis was the identification of Y-box-binding protein (YBX1), a DNA- and RNA- binding protein that has properties of a

nucleic acid chaperone [116], in 21D1-Exos (**Table 3**). YBX1 was the most up-regulated protein in exosomes following EMT (Rsc 27.5), and its unique expression in 21D1-Exos was validated by western blotting (**Fig. 2A**). YBX1is known to be involved in almost all DNA- and mRNA-dependent processes including DNA replication and repair, transcription, pre-mRNA splicing, and mRNA translation [116], and is considered to be a master transcriptional regulator. YBX1 can bind RNA to limit protein synthesis, or bind DNA through the Y-box promoter element containing an inverted CCAAT box to either activate or repress transcription [117, 118]. YBX1 is known to interact with other DNA binding proteins such as PURα (PURA), also uniquely present in 21D1-Exos (Rsc 2.6) (**Table 3**). PURα regulates cell proliferation through the activation of growth-associated gene transcription [119] [120]. MMP-13 expression is also known to be regulated by YBX1 [121], and given that MMP-13 was uniquely identified in MDCK-Exos (Rsc -79.8) it is possible that its diminished expression in 21D1-Exos is due to elevated YBX1 expression. MMP-13, also known as collagenase-3, is an ECM-degrading proteinase [122] that has been reported to be selectively down-regulated in conjunction with MMP-9, by the transcription factor SPDEF during prostate tumour metastasis [123]. Given that YBX1 is known to promote an epithelial-mesenchymal transition through translational activation of snail1, it is interesting to hypothesise that 21D1-Exos may also induce EMT via YBX1 in recipient cells [124].

(INSERT TABLE 3)

In summary, proteomic profiling of highly-purified exosomes has revealed new insights into the contribution of exosomes to the extracellular microenvironment after oncogenic H-Ras-induced EMT. We show that exosomes released from epithelial MDCK cells undergo extensive reprogramming causing exosome-mediated release of several factors associated

with modifying the extracellular tumour microenvironment including proteases, annexins, integrins and secreted ECM components. It is possible that these factors may positively feedback on themselves to maintain the EMT process, or induce neighbouring cells to undergo EMT. In addition, our findings reveal for the first time that oncogenic H-Ras transformation induces the packaging and release of mediators associated with nuclear assembly, transcription, splicing, and protein translation. Given that 21D1-Exos contain several features known to induce EMT, it is tempting to speculate that Ras-transformed exosomes are functionally capable of initiating EMT in recipient cells.

ACKNOWLEDGEMENTS

This work was supported by the National Health & Medical Research Council (NHMRC) of Australia for program grant #487922 (RJS, JH, DWG), grants #280913 and #433619 (H-JZ), grants #628946 and #400202 (AFH). AFH is also supported by an Australian Research Council (www.arc.gov.au) Future Fellowship (FT100100560). RAM is supported by an Early Career CJ Martin Fellowship #APP1037043, and BMC by an NHMRC Dora Lush Biomedical Postgraduate Scholarship #628959. BJT is supported by The University of Melbourne Research Scholarship. Analysis of proteomic data described in this work was supported using the Australian Proteomics Computational Facility funded by the National Health & Medical Research Council of Australia grant #381413. Electron microscopy was performed at the Advanced Microscopy Facility at the Bio21 Molecular Science and Biotechnology Institute, The University of Melbourne. This work was also supported, in part, by American Recovery and Reinvestment Act funds through National Institutes of Health Grant R01 HG005805 (RLM), the NIGMS Grant 2P50 GM076547 from Center for Systems

Biology, the Luxembourg Centre for Systems Biomedicine and the University of Luxembourg, and from the National Science Foundation (MRI Grant 0923536). UK was supported by a fellowship from the German Academic Exchange Service. We thank the NCI of the NIH for support (Grant #1R03CA156667 to RLM).

REFERENCES

1. Hay, E.D. (1995) An overview of epithelio-mesenchymal transformation. Acta Anatomica. 154(1). 8-20.
2. Hugo, H., Ackland, M.L., Blick, T., Lawrence, M.G., Clements, J.A., Williams, E.D., Thompson, E.W. (2007) Epithelial--mesenchymal and mesenchymal--epithelial transitions in carcinoma progression. J Cell Physiol. 213(2). 374-383.
3. Thiery, J.P. (2002) Epithelial-mesenchymal transitions in tumour progression. Nat Rev Cancer. 2(6). 442-454.
4. Thiery, J.P. and Sleeman, J.P. (2006) Complex networks orchestrate epithelial-mesenchymal transitions. Nat Rev Mol Cell Biol. 7(2). 131-142.
5. Kalluri, R. and Weinberg, R.A. (2009) The basics of epithelial-mesenchymal transition. J Clin Invest. 119(6). 1420-1428.
6. Nieto, M.A. (2011) The ins and outs of the epithelial to mesenchymal transition in health and disease. Annu Rev Cell Dev Biol. 27(347-376.
7. Radisky, D.C. (2005) Epithelial-mesenchymal transition. J Cell Sci. 118(Pt 19). 4325-4326.
8. Greenburg, G. and Hay, E.D. (1982) Epithelia suspended in collagen gels can lose polarity and express characteristics of migrating mesenchymal cells. J Cell Biol. 95(1). 333-339.
9. Trelstad, R.L., Hay, E.D., Revel, J.D. (1967) Cell contact during early morphogenesis in the chick embryo. Developmental Biology. 16(1). 78-106.
10. Kalluri, R. and Neilson, E.G. (2003) Epithelial-mesenchymal transition and its implications for fibrosis. J Clin Invest. 112(12). 1776-1784.
11. Berx, G., Raspe, E., Christofori, G., Thiery, J.P., Sleeman, J.P. (2007) Pre-EMTing metastasis? Recapitulation of morphogenetic processes in cancer. Clin Exp Metastasis. 24(8). 587-597.
12. Thompson, E.W., Newgreen, D.F., Tarin, D. (2005) Carcinoma invasion and metastasis: a role for epithelial-mesenchymal transition? Cancer Res. 65(14). 5991-5995; discussion 5995.
13. Nistico, P., Bissell, M.J., Radisky, D.C. (2012) Epithelial-mesenchymal transition: general principles and pathological relevance with special emphasis on the role of matrix metalloproteinases. Cold Spring Harb Perspect Biol. 4(2). pii: a011908.
14. Yang, J. and Weinberg, R.A. (2008) Epithelial-mesenchymal transition: at the crossroads of development and tumor metastasis. Dev Cell. 14(6). 818-829.
15. Mathias, R.A., Gopal, S.K., Simpson, R.J. (2012) Contribution of cells undergoing epithelial-mesenchymal transition to the tumour microenvironment. J Proteomics. 14(78). 545-557.
16. Pelham, R.J., Rodgers, L., Hall, I., Lucito, R., Nguyen, K.C., Navin, N., Hicks, J., Mu, D., Powers, S., Wigler, M. and Botstein, D. (2006) Identification of alterations in DNA copy number in host stromal cells during tumor progression. Proc Natl Acad Sci U S A. 103(52). 19848-19853.
17. Yang, J.D., Nakamura, I., Roberts, L.R. (2011) The tumor microenvironment in hepatocellular carcinoma: current status and therapeutic targets. Semin Cancer Biol. 21(1). 35-43.
18. Bissell, M.J. and Radisky, D. (2001) Putting tumours in context. Nat Rev Cancer. 1(1). 46-54.

19. Peinado, H., Lavotshkin, S., Lyden, D. (2011) The secreted factors responsible for pre-metastatic niche formation: old sayings and new thoughts. Semin Cancer Biol. 21(2). 139-146.
20. De Wever, O., Pauwels, P., De Craene, B., Sabbah, M., Emami, S., Redeuilh, G., Gespach, C., Bracke, M., Berx, G. (2008) Molecular and pathological signatures of epithelial-mesenchymal transitions at the cancer invasion front. Histochemistry and Cell Biology. 130(3). 481-494.
21. Karagiannis, G.S., Pavlou, M.P., Diamandis, E.P. (2010) Cancer secretomics reveal pathophysiological pathways in cancer molecular oncology. Mol Oncol. 4(6). 496-510.
22. Stastna, M. and Van Eyk, J.E. (2012) Secreted proteins as a fundamental source for biomarker discovery. Proteomics. 12(4-5). 722-735.
23. Mathias, R.A., Chen, Y.S., Wang, B., Ji, H., Kapp, E.A., Moritz, R.L., Zhu, H.J., Simpson, R.J. (2010) Extracellular remodelling during oncogenic Ras-induced epithelial-mesenchymal transition facilitates MDCK cell migration. J Proteome Res. 9(2). 1007-1019.
24. Mathias, R.A., Wang, B., Ji, H., Kapp, E.A., Moritz, R.L., Zhu, H.J., Simpson, R.J. (2009) Secretome-based proteomic profiling of Ras-transformed MDCK cells reveals extracellular modulators of epithelial-mesenchymal transition. J Proteome Res. 8(6). 2827-2837.
25. Psaila, B. and Lyden, D. (2009) The metastatic niche: adapting the foreign soil. Nat Rev Cancer. 9(4). 285-293.
26. Ratajczak, J., Wysoczynski, M., Hayek, F., Janowska-Wieczorek, A., Ratajczak, M.Z. (2006) Membrane-derived microvesicles: important and underappreciated mediators of cell-to-cell communication. Leukemia. 20(9). 1487-1495.
27. Hood, J.L., San, R.S., Wickline, S.A. (2011) Exosomes released by melanoma cells prepare sentinel lymph nodes for tumor metastasis. Cancer Res. 71(11). 3792-3801.
28. Janowska-Wieczorek, A., Marquez-Curtis, L.A., Wysoczynski, M., Ratajczak, M.Z. (2006) Enhancing effect of platelet-derived microvesicles on the invasive potential of breast cancer cells. Transfusion. 46(7). 1199-1209.
29. Janowska-Wieczorek, A., Wysoczynski, M., Kijowski, J., Marquez-Curtis, L., Machalinski, B., Ratajczak, J., Ratajczak, M.Z. (2005) Microvesicles derived from activated platelets induce metastasis and angiogenesis in lung cancer. Int J Cancer. 113(5). 752-760.
30. Al-Nedawi, K., Meehan, B., Kerbel, R.S., Allison, A.C., Rak, J. (2009) Endothelial expression of autocrine VEGF upon the uptake of tumor-derived microvesicles containing oncogenic EGFR. Proc Natl Acad Sci U S A. 106(10). 3794-3799.
31. Skog, J., Wurdinger, T., van Rijn, S., Meijer, D.H., Gainche, L., Sena-Esteves, M., Curry, W.T., Jr., Carter, B.S., Krichevsky, A.M., Breakefield, X.O. (2008) Glioblastoma microvesicles transport RNA and proteins that promote tumour growth and provide diagnostic biomarkers. Nat Cell Biol. 10(12). 1470-1476.
32. Lee, T.H., D'Asti, E., Magnus, N., Al-Nedawi, K., Meehan, B., Rak, J. (2011) Microvesicles as mediators of intercellular communication in cancer--the emerging science of cellular 'debris'. Semin Immunopathol. 33(5). 455-467.
33. Mathivanan, S., Ji, H., Simpson, R.J. (2010) Exosomes: Extracellular organelles important in intercellular communication. J Proteomics. 73(10). 1907-1920.
34. Ge, R., Tan, E., Sharghi-Namini, S., Asada, H.H. (2012) Exosomes in Cancer Microenvironment and Beyond: have we Overlooked these Extracellular Messengers? Cancer Microenviron. 5(3). 323-332.

35. Hendrix, A. and Hume, A.N. (2011) Exosome signaling in mammary gland development and cancer. Int J Dev Biol. 55(7-9). 879-887.
36. Kharaziha, P., Ceder, S., Li, Q., Panaretakis, T. (2012) Tumor cell-derived exosomes: A message in a bottle. Biochim Biophys Acta. 1826(1). 103-111.
37. Yang, C. and Robbins, P.D. (2011) The roles of tumor-derived exosomes in cancer pathogenesis. Clin Dev Immunol. 2011(842849.
38. Putz, U., Howitt, J., Doan, A., Goh, C.P., Low, L.H., Silke, J., Tan, S.S. (2012) The tumor suppressor PTEN is exported in exosomes and has phosphatase activity in recipient cells. Sci Signal. 5(243). ra70.
39. Madin, S.H., Andriese, P.C., Darby, N.B. (1957) The in vitro cultivation of tissues of domestic and laboratory animals. Am J Vet Res. 18(69). 932-941.
40. Tauro, B.J., Greening, D.W., Mathias, R.A., Ji, H., Mathivanan, S., Scott, A.M., Simpson, R.J. (2012) Comparison of ultracentrifugation, density gradient separation, and immunoaffinity capture methods for isolating human colon cancer cell line LIM1863-derived exosomes. Methods. 56(2). 293-304.
41. Schroder, M., Schafer, R., Friedl, P. (1997) Spectrophotometric determination of iodixanol in subcellular fractions of mammalian cells. Anal Biochem. 244(1). 174-176.
42. Steinberg, T.H., Lauber, W.M., Berggren, K., Kemper, C., Yue, S., Patton, W.F. (2000) Fluorescence detection of proteins in sodium dodecyl sulfate-polyacrylamide gels using environmentally benign, nonfixative, saline solution. Electrophoresis. 21(3). 497-508.
43. White, I.R., Pickford, R., Wood, J., Skehel, J.M., Gangadharan, B., Cutler, P. (2004) A statistical comparison of silver and SYPRO Ruby staining for proteomic analysis. Electrophoresis. 25(17). 3048-3054.
44. Tauro, B.J., Greening, D.W., Mathias, R.A., Mathivanan, S., Ji, H., Simpson, R.J. (2012) Two distinct populations of exosomes are released from LIM1863 colon carcinoma cell-derived organoids. Mol Cell Proteomics. 12(3). 587-598.
45. Simpson, R.J., Connolly, L.M., Eddes, J.S., Pereira, J.J., Moritz, R.L., Reid, G.E. (2000) Proteomic analysis of the human colon carcinoma cell line (LIM 1215): development of a membrane protein database. Electrophoresis. 21(9). 1707-1732.
46. Olsen, J.V., de Godoy, L.M., Li, G., Macek, B., Mortensen, P., Pesch, R., Makarov, A., Lange, O., Horning, S., Mann, M. (2005) Parts per million mass accuracy on an Orbitrap mass spectrometer via lock mass injection into a C-trap. Mol Cell Proteomics. 4(12). 2010-2021.
47. Deutsch, E.W., Lam, H., Aebersold, R. (2008) PeptideAtlas: a resource for target selection for emerging targeted proteomics workflows. EMBO Rep. 9(5). 429-434.
48. Desiere, F., Deutsch, E.W., King, N.L., Nesvizhskii, A.I., Mallick, P., Eng, J., Chen, S., Eddes, J., Loevenich, S.N., Aebersold, R. (2006) The PeptideAtlas project. Nucleic Acids Res. 34(Database issue). D655-658.
49. Desiere, F., Deutsch, E.W., Nesvizhskii, A.I., Mallick, P., King, N.L., Eng, J.K., Aderem, A., Boyle, R., Brunner, E., Donohoe, S., Fausto, N., Hafen, E., Hood, L., Katze, M.G., Kennedy, K.A., Kregenow, F., Lee, H., Lin, B., Martin, D., Ranish, J.A., Rawlings, D.J., Samelson, L.E., Shiio, Y., Watts, J.D., Wollscheid, B., Wright, M.E., Yan, W., Yang, L., Yi, E.C., Zhang, H. and Aebersold, R. (2005) Integration with the human genome of peptide sequences obtained by high-throughput mass spectrometry. Genome Biol. 6(1). R9.
50. Greening, D.W., Glenister, K.M., Kapp, E.A., Moritz, R.L., Sparrow, R.L., Lynch, G.W., Simpson, R.J. (2008) Comparison of human platelet membrane-cytoskeletal

proteins with the plasma proteome: Towards understanding the platelet-plasma nexus. Proteomics Clin Appl. 2(1). 63-77.

51. Chen, Y.S., Mathias, R.A., Mathivanan, S., Kapp, E.A., Moritz, R.L., Zhu, H.J., Simpson, R.J. (2011) Proteomics profiling of Madin-Darby canine kidney plasma membranes reveals Wnt-5a involvement during oncogenic H-Ras/TGF-beta-mediated epithelial-mesenchymal transition. Mol Cell Proteomics. 10(2). M110 001131.
52. Beissbarth, T., Hyde, L., Smyth, G.K., Job, C., Boon, W.M., Tan, S.S., Scott, H.S., Speed, T.P. (2004) Statistical modeling of sequencing errors in SAGE libraries. Bioinformatics. 20 Suppl 1(i31-39.
53. Old, W.M., Meyer-Arendt, K., Aveline-Wolf, L., Pierce, K.G., Mendoza, A., Sevinsky, J.R., Resing, K.A., Ahn, N.G. (2005) Comparison of label-free methods for quantifying human proteins by shotgun proteomics. Mol Cell Proteomics. 4(10). 1487-1502.
54. Benjamini, Y. and Hochberg, Y. (1995) Controlling the false discovery rate: a practical and powerful approach to multiple testing. J. R. Stat. Soc. Ser. B-Stat. Methodol. 57(1). 289-300.
55. Team, R.D.C. *R: A language and environment for statistical computing*, in *R Foundation for Statistical Computing*, 2008: Vienna, Austria. p. ISBN 3-900051-900007-900050.
56. Demory Beckler, M., Higginbotham, J.N., Franklin, J.L., Ham, A.J., Halvey, P.J., Imasuen, I.E., Whitwell, C., Li, M., Liebler, D.C., Coffey, R.J. (2013) Proteomic Analysis of Exosomes from Mutant KRAS Colon Cancer Cells Identifies Intercellular Transfer of Mutant KRAS. Molecular & cellular proteomics : MCP. 12(2). 343-355.
57. Simpson, R.J., Lim, J.W., Moritz, R.L., Mathivanan, S. (2009) Exosomes: proteomic insights and diagnostic potential. Expert Rev Proteomics. 6(3). 267-283.
58. Nazarenko, I., Rana, S., Baumann, A., McAlear, J., Hellwig, A., Trendelenburg, M., Lochnit, G., Preissner, K.T., Zoller, M. (2010) Cell surface tetraspanin Tspan8 contributes to molecular pathways of exosome-induced endothelial cell activation. Cancer Res. 70(4). 1668-1678.
59. Rana, S. and Zoller, M. (2011) Exosome target cell selection and the importance of exosomal tetraspanins: a hypothesis. Biochem Soc Trans. 39(2). 559-562.
60. Fukuda, M. (2008) Regulation of secretory vesicle traffic by Rab small GTPases. Cell Mol Life Sci. 65(18). 2801-2813.
61. Lee, M.T., Mishra, A., Lambright, D.G. (2009) Structural mechanisms for regulation of membrane traffic by rab GTPases. Traffic. 10(10). 1377-1389.
62. Stenmark, H. (2009) Rab GTPases as coordinators of vesicle traffic. Nat Rev Mol Cell Biol. 10(8). 513-525.
63. Thery, C., Ostrowski, M., Segura, E. (2009) Membrane vesicles as conveyors of immune responses. Nat Rev Immunol. 9(8). 581-593.
64. Kalra, H., Simpson, R.J., Ji, H., Aikawa, E., Altevogt, P., Askenase, P., Bond, V.C., Borras, F.E., Breakefield, X., Budnik, V., Buzas, E., Camussi, G., Clayton, A., Cocucci, E., Falcon-Perez, J.M., Gabrielsson, S., Gho, Y.S., Gupta, D., Harsha, H.C., Hendrix, A., Hill, A.F., Inal, J.M., Jenster, G., Kramer-Albers, E.M., Lim, S.K., Llorente, A., Lotvall, J., Marcilla, A., Mincheva-Nilsson, L., Nazarenko, I., Nieuwland, R., Nolte-'t Hoen, E.N., Pandey, A., Patel, T., Piper, M.G., Pluchino, S., Prasad, T.S., Rajendran, L., Raposo, G., Record, M., Reid, G.E., Sanchez-Madrid, F., Schiffelers, R.M., Siljander, P., Stensballe, A., Stoorvogel, W., Taylor, D., Thery, C., Valadi, H., van Balkom, B.W., Vazquez, J., Vidal, M., Wauben, M.H., Yanez-Mo, M., Zoeller, M. and Mathivanan, S. (2012) Vesiclepedia: a compendium for

extracellular vesicles with continuous community annotation. PLoS Biol. 10(12). e1001450.
65. Mathivanan, S. and Simpson, R.J. (2009) ExoCarta: A compendium of exosomal proteins and RNA. Proteomics. 9(21). 4997-5000.
66. Peinado, H., Aleckovic, M., Lavotshkin, S., Matei, I., Costa-Silva, B., Moreno-Bueno, G., Hergueta-Redondo, M., Williams, C., Garcia-Santos, G., Ghajar, C., Nitadori-Hoshino, A., Hoffman, C., Badal, K., Garcia, B.A., Callahan, M.K., Yuan, J., Martins, V.R., Skog, J., Kaplan, R.N., Brady, M.S., Wolchok, J.D., Chapman, P.B., Kang, Y., Bromberg, J. and Lyden, D. (2012) Melanoma exosomes educate bone marrow progenitor cells toward a pro-metastatic phenotype through MET. Nature Med. 18(6). 883-891.
67. Kaplan, R.N., Riba, R.D., Zacharoulis, S., Bramley, A.H., Vincent, L., Costa, C., MacDonald, D.D., Jin, D.K., Shido, K., Kerns, S.A., Zhu, Z., Hicklin, D., Wu, Y., Port, J.L., Altorki, N., Port, E.R., Ruggero, D., Shmelkov, S.V., Jensen, K.K., Rafii, S. and Lyden, D. (2005) VEGFR1-positive haematopoietic bone marrow progenitors initiate the pre-metastatic niche. Nature. 438(7069). 820-827.
68. Sleeman, J.P. (2012) The metastatic niche and stromal progression. Cancer metastasis reviews. 31(3-4). 429-440.
69. Nguyen, D.X., Bos, P.D., Massague, J. (2009) Metastasis: from dissemination to organ-specific colonization. Nature reviews. Cancer. 9(4). 274-284.
70. Psaila, B. and Lyden, D. (2009) The metastatic niche: adapting the foreign soil. Nature reviews. Cancer. 9(4). 285-293.
71. Khamis, Z.I., Sahab, Z.J., Sang, Q.X. (2012) Active roles of tumor stroma in breast cancer metastasis. Int J Breast Cancer. Epub Feb 19.
72. Castellana, D., Zobairi, F., Martinez, M.C., Panaro, M.A., Mitolo, V., Freyssinet, J.M., Kunzelmann, C. (2009) Membrane microvesicles as actors in the establishment of a favorable prostatic tumoral niche: a role for activated fibroblasts and CX3CL1-CX3CR1 axis. Cancer Res. 69(3). 785-793.
73. Jung, T., Castellana, D., Klingbeil, P., Cuesta Hernandez, I., Vitacolonna, M., Orlicky, D.J., Roffler, S.R., Brodt, P., Zoller, M. (2009) CD44v6 dependence of premetastatic niche preparation by exosomes. Neoplasia. 11(10). 1093-1105.
74. Grange, C., Tapparo, M., Collino, F., Vitillo, L., Damasco, C., Deregibus, M.C., Tetta, C., Bussolati, B., Camussi, G. (2011) Microvesicles released from human renal cancer stem cells stimulate angiogenesis and formation of lung premetastatic niche. Cancer Res. 71(15). 5346-5356.
75. Kenny, P.A., Lee, G.Y., Bissell, M.J. (2007) Targeting the tumor microenvironment. Frontiers in bioscience : a journal and virtual library. 12, 3468-3474.
76. Kang, Y., Siegel, P.M., Shu, W., Drobnjak, M., Kakonen, S.M., Cordon-Cardo, C., Guise, T.A., Massague, J. (2003) A multigenic program mediating breast cancer metastasis to bone. Cancer Cell. 3(6). 537-549.
77. Nicoloso, M.S., Spizzo, R., Shimizu, M., Rossi, S., Calin, G.A. (2009) MicroRNAs--the micro steering wheel of tumour metastases. Nat Rev Cancer. 9(4). 293-302.
78. Pulukuri, S.M. and Rao, J.S. (2008) Matrix metalloproteinase-1 promotes prostate tumor growth and metastasis. Int J Oncol. 32(4). 757-765.
79. Shiozawa, J., Ito, M., Nakayama, T., Nakashima, M., Kohno, S., Sekine, I. (2000) Expression of matrix metalloproteinase-1 in human colorectal carcinoma. Mod Pathol. 13(9). 925-933.
80. Itoh, Y. and Seiki, M. (2006) MT1-MMP: a potent modifier of pericellular microenvironment. J Cell Physiol. 206(1). 1-8.

81. Muller, M., Beck, I.M., Gadesmann, J., Karschuk, N., Paschen, A., Proksch, E., Djonov, V., Reiss, K., Sedlacek, R. (2010) MMP19 is upregulated during melanoma progression and increases invasion of melanoma cells. Mod Pathol. 23(4). 511-521.
82. Nakahara, H., Howard, L., Thompson, E.W., Sato, H., Seiki, M., Yeh, Y., Chen, W.T. (1997) Transmembrane/cytoplasmic domain-mediated membrane type 1-matrix metalloprotease docking to invadopodia is required for cell invasion. Proc Natl Acad Sci U S A. 94(15). 7959-7964.
83. Rocks, N., Paulissen, G., El Hour, M., Quesada, F., Crahay, C., Gueders, M., Foidart, J.M., Noel, A., Cataldo, D. (2008) Emerging roles of ADAM and ADAMTS metalloproteinases in cancer. Biochimie. 90(2). 369-379.
84. Murphy, G. (2008) The ADAMs: signalling scissors in the tumour microenvironment. Nat Rev Cancer. 8(12). 929-941.
85. Gutwein, P., Mechtersheimer, S., Riedle, S., Stoeck, A., Gast, D., Joumaa, S., Zentgraf, H., Fogel, M., Altevogt, D.P. (2003) ADAM10-mediated cleavage of L1 adhesion molecule at the cell surface and in released membrane vesicles. Faseb J. 17(2). 292-294.
86. Porter, S., Clark, I.M., Kevorkian, L., Edwards, D.R. (2005) The ADAMTS metalloproteinases. Biochem J. 386(Pt 1). 15-27.
87. Liu, Y.J., Xu, Y., Yu, Q. (2006) Full-length ADAMTS-1 and the ADAMTS-1 fragments display pro- and antimetastatic activity, respectively. Oncogene. 25(17). 2452-2467.
88. Guise, T.A. (2009) Breaking down bone: new insight into site-specific mechanisms of breast cancer osteolysis mediated by metalloproteinases. Genes Dev. 23(18). 2117-2123.
89. Guo, W. and Giancotti, F.G. (2004) Integrin signalling during tumour progression. Nat Rev Mol Cell Biol. 5(10). 816-826.
90. Ahmed, N., Riley, C., Rice, G., Quinn, M. (2005) Role of integrin receptors for fibronectin, collagen and laminin in the regulation of ovarian carcinoma functions in response to a matrix microenvironment. Clin Exp Metastasis. 22(5). 391-402.
91. Munger, J.S., Huang, X., Kawakatsu, H., Griffiths, M.J., Dalton, S.L., Wu, J., Pittet, J.F., Kaminski, N., Garat, C., Matthay, M.A., Rifkin, D.B. and Sheppard, D. (1999) The integrin alpha v beta 6 binds and activates latent TGF beta 1: a mechanism for regulating pulmonary inflammation and fibrosis. Cell. 96(3). 319-328.
92. Hemler, M.E. (2005) Tetraspanin functions and associated microdomains. Nat Rev Mol Cell Biol. 6(10). 801-811.
93. Bassani, S. and Cingolani, L.A. (2012) Tetraspanins: Interactions and interplay with integrins. Int J Biochem Cell Biol. 44(5). 703-708.
94. Wang, H.X., Li, Q., Sharma, C., Knoblich, K., Hemler, M.E. (2011) Tetraspanin protein contributions to cancer. Biochem Soc Trans. 39(2). 547-552.
95. Domanico, S.Z., Pelletier, A.J., Havran, W.L., Quaranta, V. (1997) Integrin alpha 6A beta 1 induces CD81-dependent cell motility without engaging the extracellular matrix migration substrate. Mol Biol Cell. 8(11). 2253-2265.
96. Luga, V., Zhang, L., Viloria-Petit, A.M., Ogunjimi, A.A., Inanlou, M.R., Chiu, E., Buchanan, M., Hosein, A.N., Basik, M., Wrana, J.L. (2012) Exosomes Mediate Stromal Mobilization of Autocrine Wnt-PCP Signaling in Breast Cancer Cell Migration. Cell. 151(7). 1542-1556.
97. He, B., Liu, L., Cook, G.A., Grgurevich, S., Jennings, L.K., Zhang, X.A. (2005) Tetraspanin CD82 attenuates cellular morphogenesis through down-regulating integrin alpha6-mediated cell adhesion. J Biol Chem. 280(5). 3346-3354.

98. Fei, Y., Wang, J., Liu, W., Zuo, H., Qin, J., Wang, D., Zeng, H., Liu, Z. (2012) CD151 promotes cancer cell metastasis via integrins alpha3beta1 and alpha6beta1 in vitro. Mol Med Rep. 6(6). 1226-1230.
99. Gerke, V., Creutz, C.E., Moss, S.E. (2005) Annexins: linking Ca2+ signalling to membrane dynamics. Nat Rev Mol Cell Biol. 6(6). 449-461.
100. Sharma, M.R., Koltowski, L., Ownbey, R.T., Tuszynski, G.P., Sharma, M.C. (2006) Angiogenesis-associated protein annexin II in breast cancer: selective expression in invasive breast cancer and contribution to tumor invasion and progression. Exp Mol Pathol. 81(2). 146-156.
101. Bao, H., Jiang, M., Zhu, M., Sheng, F., Ruan, J., Ruan, C. (2009) Overexpression of Annexin II affects the proliferation, apoptosis, invasion and production of proangiogenic factors in multiple myeloma. Int J Hematol. 90(2). 177-185.
102. Shapiro, I.M., Cheng, A.W., Flytzanis, N.C., Balsamo, M., Condeelis, J.S., Oktay, M.H., Burge, C.B., Gertler, F.B. (2011) An EMT-driven alternative splicing program occurs in human breast cancer and modulates cellular phenotype. PLoS Genet. 7(8). e1002218.
103. Moreno-Bueno, G., Portillo, F., Cano, A. (2008) Transcriptional regulation of cell polarity in EMT and cancer. Oncogene. 27(55). 6958-6969.
104. Brown, R.L., Reinke, L.M., Damerow, M.S., Perez, D., Chodosh, L.A., Yang, J., Cheng, C. (2011) CD44 splice isoform switching in human and mouse epithelium is essential for epithelial-mesenchymal transition and breast cancer progression. J Clin Invest. 121(3). 1064-1074.
105. Warzecha, C.C., Jiang, P., Amirikian, K., Dittmar, K.A., Lu, H., Shen, S., Guo, W., Xing, Y., Carstens, R.P. (2010) An ESRP-regulated splicing programme is abrogated during the epithelial-mesenchymal transition. Embo J. 29(19). 3286-3300.
106. Biamonti, G., Bonomi, S., Gallo, S., Ghigna, C. (2012) Making alternative splicing decisions during epithelial-to-mesenchymal transition (EMT). Cell Mol Life Sci. 69(15). 2515-2526.
107. Savagner, P., Valles, A.M., Jouanneau, J., Yamada, K.M., Thiery, J.P. (1994) Alternative splicing in fibroblast growth factor receptor 2 is associated with induced epithelial-mesenchymal transition in rat bladder carcinoma cells. Mol Biol Cell. 5(8). 851-862.
108. Wu, C.Y., Tsai, Y.P., Wu, M.Z., Teng, S.C., Wu, K.J. (2012) Epigenetic reprogramming and post-transcriptional regulation during the epithelial-mesenchymal transition. Trends Genet. 28(9). 454-463.
109. Warzecha, C.C. and Carstens, R.P. (2012) Complex changes in alternative pre-mRNA splicing play a central role in the epithelial-to-mesenchymal transition (EMT). Semin Cancer Biol. 22(5-6). 417-427.
110. Wahl, M.C., Will, C.L., Luhrmann, R. (2009) The spliceosome: design principles of a dynamic RNP machine. Cell. 136(4). 701-718.
111. Ghigna, C., Giordano, S., Shen, H., Benvenuto, F., Castiglioni, F., Comoglio, P.M., Green, M.R., Riva, S., Biamonti, G. (2005) Cell motility is controlled by SF2/ASF through alternative splicing of the Ron protooncogene. Mol Cell. 20(6). 881-890.
112. Lu, Y., Yao, H.P., Wang, M.H. (2007) Multiple variants of the RON receptor tyrosine kinase: biochemical properties, tumorigenic activities, and potential drug targets. Cancer Lett. 257(2). 157-164.
113. Valacca, C., Bonomi, S., Buratti, E., Pedrotti, S., Baralle, F.E., Sette, C., Ghigna, C., Biamonti, G. (2010) Sam68 regulates EMT through alternative splicing-activated nonsense-mediated mRNA decay of the SF2/ASF proto-oncogene. J Cell Biol. 191(1). 87-99.

114. Collesi, C., Santoro, M.M., Gaudino, G., Comoglio, P.M. (1996) A splicing variant of the RON transcript induces constitutive tyrosine kinase activity and an invasive phenotype. Mol Cell Biol. 16(10). 5518-5526.
115. Karni, R., de Stanchina, E., Lowe, S.W., Sinha, R., Mu, D., Krainer, A.R. (2007) The gene encoding the splicing factor SF2/ASF is a proto-oncogene. Nat Struct Mol Biol. 14(3). 185-193.
116. Eliseeva, I.A., Kim, E.R., Guryanov, S.G., Ovchinnikov, L.P., Lyabin, D.N. (2011) Y-box-binding protein 1 (YB-1) and its functions. Biochemistry (Mosc). 76(13). 1402-1433.
117. Bader, A.G. and Vogt, P.K. (2004) An essential role for protein synthesis in oncogenic cellular transformation. Oncogene. 23(18). 3145-3150.
118. Kohno, K., Izumi, H., Uchiumi, T., Ashizuka, M., Kuwano, M. (2003) The pleiotropic functions of the Y-box-binding protein, YB-1. Bioessays. 25(7). 691-698.
119. Lasham, A., Lindridge, E., Rudert, F., Onrust, R., Watson, J. (2000) Regulation of the human fas promoter by YB-1, Puralpha and AP-1 transcription factors. Gene. 252(1-2). 1-13.
120. Ladomery, M. and Sommerville, J. (1995) A role for Y-box proteins in cell proliferation. Bioessays. 17(1). 9-11.
121. Samuel, S., Beifuss, K.K., Bernstein, L.R. (2007) YB-1 binds to the MMP-13 promoter sequence and represses MMP-13 transactivation via the AP-1 site. Biochim Biophys Acta. 1769(9-10). 525-531.
122. Knauper, V., Lopez-Otin, C., Smith, B., Knight, G., Murphy, G. (1996) Biochemical characterization of human collagenase-3. J Biol Chem. 271(3). 1544-1550.
123. Steffan, J.J., Koul, S., Meacham, R.B., Koul, H.K. (2012) The transcription factor SPDEF suppresses prostate tumor metastasis. J Biol Chem. 287(35). 29968-29978.
124. Evdokimova, V., Tognon, C., Ng, T., Ruzanov, P., Melnyk, N., Fink, D., Sorokin, A., Ovchinnikov, L.P., Davicioni, E., Triche, T.J. and Sorensen, P.H. (2009) Translational activation of snail1 and other developmentally regulated transcription factors by YB-1 promotes an epithelial-mesenchymal transition. Cancer Cell. 15(5). 402-415.

FIGURE LEGENDS

Figure 1. **Isolation of exosomes released from MDCK and 21D1 cells**. (A) Phase contrast images of MDCK cells reveal epithelial cobblestone-like morphology, while 21D1 cells display an elongated mesenchymal-like spindle shape. (B) Experimental workflow for MDCK and 21D1-Exos isolation.

Figure 2. **Characterisation of MDCK- and 21D1-Exos**. (A) For Western blotting, exosome preparations (10 µg) were separated by 1D-SDS-PAGE, electrotransferred, and probed with exosome markers Alix and TSG101. Additionally, exosomes were probed with epithelial cell markers CDH1 (E-Cadherin) and EpCAM revealing a downregulation in 21D1-Exos as compared to MDCK-Exos. HRAS (H-Ras), VIM (vimentin) MMP1 (interstitial collagenase) and YBX1 were significantly enriched in 21D1-Exos. (B) MDCK- and 21D1-Exos were imaged using cryo-electron microscopy to reveal textured round vesicles between 40-100 nm. Scale bar, 100 nm.

Figure 3. **Proteomic analysis of exosomes**. (A) MDCK- and 21D1-Exos proteins were separated by 1D-SDS-PAGE and stained with Imperial^{TM} Protein Stain. Individual gel slices were excised and subjected to in-gel reduction, alkylation, and tryptic digestion. Extracted peptides were separated by reverse phase–high performance liquid chromatography (RP-HPLC) followed by mass spectrometry analysis, database searching and protein annotation. (B) A two-way Venn diagram of MDCK- and 21D1-Exos reveals 325 proteins were commonly identified, while 57 and 76 proteins were uniquely identified in MDCK- and 21D1-Exos, respectively (Supplemental Tables S1-3).

Table 1. EMT hallmark proteins identified in MDCK- and 21D1-Exos

Category[a]	Gene Name	Protein Description	Spectral counts[b]		Protein abundance ratio[c]
			MDCK-Exos	21D1-Exos	
Cell-cell contact	THBS1	Thrombospondin-1	555		-482.8*
	CDH1	E-cadherin	41		-34.4*
	EPCAM	Epithelial cell adhesion molecule	19		-16.5*
Cell-matrix contact	COL12A1	Collagen alpha-1(XII) chain	90		-74.8*
	LAMA3	Laminin subunit alpha-3	83		-69.0*
	LAMB3	Laminin beta 3	56		-46.7*
	LAMC2	Laminin-5 gamma 2	61	1	-28.2*
	COL5A1	Collagen alpha-1(V) chain	15		-13.2*
	LAMC1	Laminin subunit gamma-1	91	11	-7.7*
	HSPG2	Perlecan	1325	211	-7.3*
	LAMB1	Laminin subunit beta-1	89	13	-6.5*
	LAMB2	Laminin subunit beta-2	6		-5.9
	COL17A1	Collagen alpha-1(XVII) chain	9	1	-4.6*
Cell polarity	MUC1	Endometrial mucin-1	24		-20.5*
	CLDN3	Claudin-3	10	2	-3.5
	CLDN4	Claudin-4	12	3	-3.2
	CLDN6	Claudin-6	7	5	-1.3
Cytoskeleton Remodeling	RHOA	Transforming protein RhoA	2	5	1.9
	VIM	Vimentin		9	8.1*
Proteases	MMP1	Interstitial collagenase		8	7.3*
	MMP14	Matrix metalloproteinase-14		3	3.4
	MMP19	Matrix metalloproteinase-19		13	11.3*
	ADAMTS1	A disintegrin and metalloproteinase with thrombospondin motifs 1	4	8	1.7
	ADAM10	ADAM-10	12	28	2.2

[a] Category based on reference [5-7, 13, 90].

[b] Significant protein spectral counts (SpC) where a peptide spectrum is deemed significant when the Ion score ≥ the Homology score (refer Supplemental Table S1)

[c] Protein abundance ratio (ratio of spectral counts; Rsc) reveals differential protein abundance between MDCK- and 21D1-Exos based on Eq.1. The use of zero spectra is overcome using an arbitrary correction factor (1.25) in Eq. 1. The use of this correction factor allows relative quantitation of all proteins within both normalized datasets to be performed, based upon Old et al. [53]. Positive Rsc values reflect increased protein abundance in 21D1-Exos relative to MDCK-Exos; negative values indicate decreased abundance in 21D1-Exos relative to MDCK-Exos.

* Differential expression with p-values <0.05 as reported in Supplemental Table S1

Table 2. Exosomal factors involved in metastatic niche formation and metastasis

Category[a]	Gene Name	Protein Description	Spectral counts[b]		Protein abundance ratio[c]
			MDCK-Exos	21D1-Exos	
Proteases	MMP1	Interstitial collagenase		8	7.3*
	MMP14	Matrix metalloproteinase-14		3	3.4
	MMP19	Matrix metalloproteinase-19		13	11.3*
	ADAM10	ADAM-10	12	28	2.2
	ADAMTS1	A disintegrin and metalloproteinase with thrombospondin motifs 1	4	8	1.7
Integrins	ITGB1	Integrin beta-1	44	191	4.3*
	ITGA3	Integrin alpha-3	18	105	5.5*
	ITGAV	Integrin alpha-V	6	23	3.3*
	ITGA6	Integrin alpha-6		9	8.1*
Tetraspanins	CD81	CD81	10	13	1.25
	CD82	CD82 antigen	2	6	3.25
	CD151	CD151 antigen	4	21	4.19*
Annexins	ANXA1	Annexin A1	14	19	1.3
	ANXA2	Annexin A2	12	24	1.9
	ANXA4	Annexin A4	2	3	1.3
	ANXA7	Annexin A7	2	3	1.3
	ANXA8	Annexin A8	1	4	2.3
	ANXA11	Annexin A11	8	11	1.3

[a] Category based on references [13, 19, 27, 66, 75, 76, 89, 96, 100].

[b] Significant protein spectral counts (SpC) where a peptide spectrum is deemed significant when the Ion score ≥ the Homology score (refer Supplemental Table S1)

[c] Protein abundance ratio (ratio of spectral counts; Rsc) reveals differential protein abundance between MDCK- and 21D1-Exos based on Eq.1. The use of zero spectra is overcome using an arbitrary correction factor (1.25) in Eq. 1. The use of this correction factor allows relative quantitation of all proteins within both normalized datasets to be performed, based upon Old et al. [53]. Positive Rsc values reflect increased protein abundance in 21D1-Exos relative to MDCK-Exos; negative values indicate decreased abundance in 21D1-Exos relative to MDCK-Exos.

* Differential expression with p-values <0.05 as reported in Supplemental Table S1

Table 3. Splicing factors and transcription factors enriched in 21D1-Exos

Category[a]	Gene Name	Protein Description	Spectral counts[b]		Protein abundance ratio[c]
			MDCK-Exos	21D1-Exos	
Splicing Factors	SF3B1	Splicing factor 3B subunit 1		10	8.9*
	SF3B3	Splicing factor 3B subunit 3		2	2.6
	SFRS1	Splicing factor, arginine/serine-rich 1		28	23.2*
	SRP20	Serine/arginine-rich splicing factor 3	1	5	2.7
Transcription Factors	PURA	Transcriptional activator protein Pur-alpha		2	2.6
	NCL	Nucleolin		28	23.2*
	YBX1	Nuclease-sensitive element-binding protein 1		46	37.5*
Other	EHD2	EH domain-containing protein 2		35	28.7*

[a] Category based on reference [102, 103, 111, 116]

[b] Significant protein spectral counts (SpC) where a peptide spectrum is deemed significant when the Ion score ≥ the Homology score (refer Supplemental Table S1)

[c] Protein abundance ratio (ratio of spectral counts; Rsc) reveals differential protein abundance between MDCK- and 21D1-Exos based on Eq.1. The use of zero spectra is overcome using an arbitrary correction factor (1.25) in Eq. 1. The use of this correction factor allows relative quantitation of all proteins within both normalized datasets to be performed, based upon Old et al. [53]. Positive Rsc values reflect increased protein abundance in 21D1-Exos relative to MDCK-Exos; negative values indicate decreased abundance in 21D1-Exos relative to MDCK-Exos.

* Differential expression with p-values <0.05 as reported in Supplemental Table S1

FIGURES

Figure 1

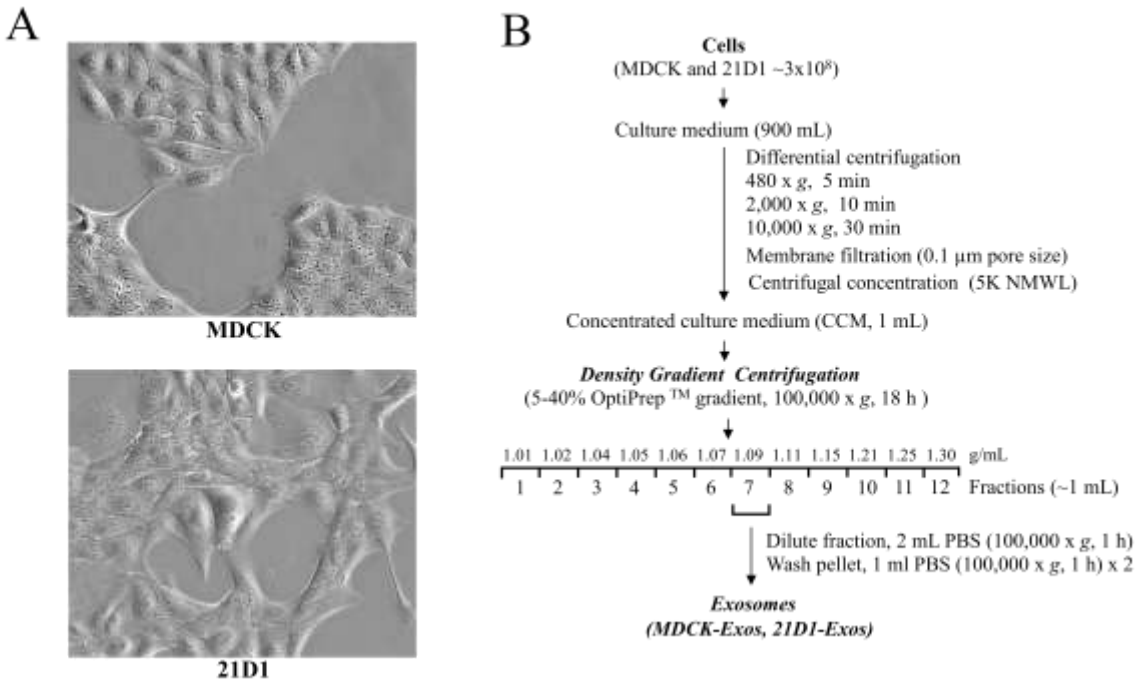

Figure 2

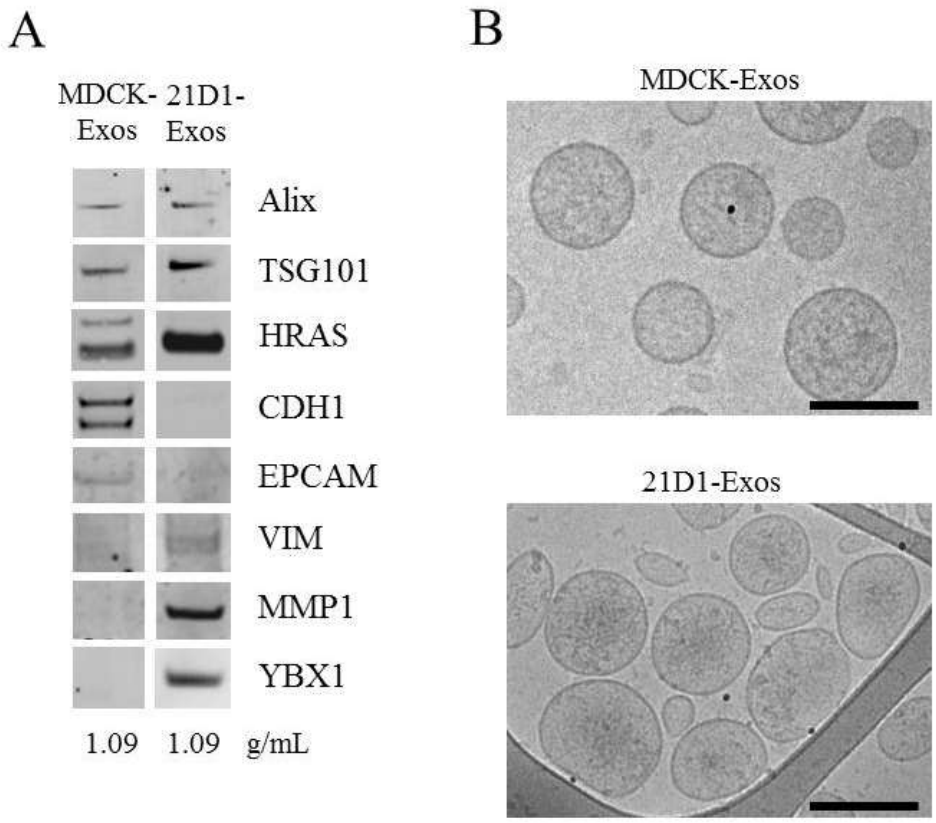
A
MDCK-Exos
21D1-Exos
Alix
TSG101
HRAS
CDH1
EPCAM
VIM
MMP1
YBX1
1.09
1.09
g/mL
B
MDCK-Exos
21D1-Exos

Figure 3

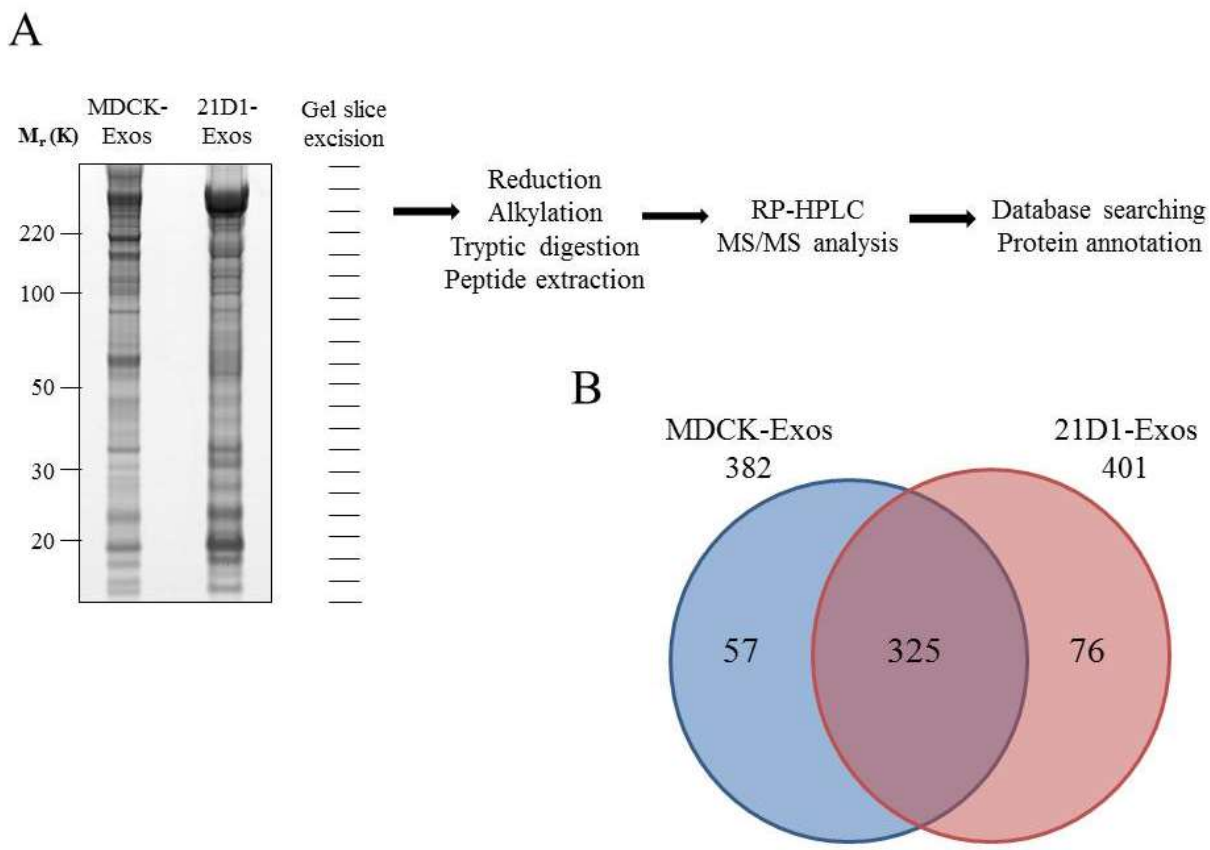
A
MDCK-Exos
21D1-Exos
Gel slice excision
M_r (K)
220
100
50
30
20
Reduction
Alkylation
Tryptic digestion
Peptide extraction
RP-HPLC
MS/MS analysis
Database searching
Protein annotation
B
MDCK-Exos
382
21D1-Exos
401
57
325
76